

CT diagnosis and differentiation of benign and malignant varieties of solitary fibrous tumor of the pleura

Xiaofang You, MD^a, Xiwen Sun, MD^a, Chunyan Yang, MD^b, Yong Fang, MD^{c,*}

Abstract

To investigate computed tomography (CT) characteristics of benign and malignant solitary fibrous tumors of the pleura (SFTPs). Preoperative CTs for 60 SFTP cases (49 benign and 11 malignant) with subsequently confirmed diagnoses were retrospectively analyzed.

Tumor morphologies included mounded or mushroom umbrella-shape (19 cases, 31.7%), quasi-circular or oval-shape (30 cases, 50%), and growth resembling a casting mould (12 cases, 20%). Maximum tumor diameters were 1.1 to 18.9 cm (average: 6.4 ± 4.8 cm). Fifty-seven cases had clear boundaries, and 3 had partially coarse boundaries. Twenty-seven cases showed homogeneous density; 33, "geographic"-patterned inhomogeneous density; 6, calcifications; 12, intratumor blood vessels; and 3, thick nourishing peritumoral blood vessels. Pleural thickening (regular and irregular) was found adjacent to tumors in 4, compression of adjacent ribs with absorption and cortical sclerosis in 2, and location adjacent to ribs with bony destruction in 1. Four cases had a small amount of lung tissue enfolded along the boundary, 2 had multiple peritumoral pulmonary bullae, and 9 had small ipsilateral pleural effusions. Compared with benign and malignant SFTPs were larger ($P < .001$), had inhomogeneous density, and were more commonly associated with intratumor blood vessels and pleural effusions ($P < .01$).

CT revealed characteristic patterns in SFTPs, including casting mould-like growth, rich blood supply, and "geographic"-patterned enhancement. In addition, larger tumor size, inhomogeneous intensities, abundant intratumor blood vessels, and pleural effusions were more common with malignancy. Lastly, multislice CT angiography can reveal feeding arteries and help guide surgical management.

Abbreviations: CT = computed tomography, MIP = maximum density projection, MPR = multiplanar reconstruction, MSCT = multislice computed tomography, MSFP = malignant solitary fibrous tumor of the pleura, SFT = solitary fibrous tumor, SFTP = solitary fibrous tumor of the pleura, VR = volume rendering.

Keywords: benign, computed tomography, malignant, solitary fibrous tumor of the pleura, X-ray

1. Introduction

A solitary fibrous tumor (SFT) is a rare mesenchymal tumor that can occur in any part of the body. In the chest cavity, it is called a solitary fibrous tumor of the pleura (SFTP).^[1,2] A pleural tumor was first mentioned by Lieutaud in 1767, and the concept was put

forward again by Wagner in 1870; Klemperer et al were the first to provide a pathologic description in 1931.

With the development of pathology, immunohistochemistry, and imaging techniques, the understanding of SFTP has improved. Reports on this tumor type have gradually increased, but the etiology remains unknown. It is now known that SFTP arises from CD34-positive dendritic mesenchymal cells, is a benign or low-grade malignant tumor, and accounts for <5% of all pleural tumors. Approximately 80% of SFTPs arise from the visceral pleura, and 20% from the parietal pleura. This type of tumor is often found as a solitary nodule or mass with clear boundaries, but may be lobulated; most have a capsule, and some are pedunculated with a stalk that connects to the pleura.^[3,4] It has a diverse pathology characterized by a dense circular or fusiform tumor cell zone and a rich, thick collagen fiber zone with glassy degeneration. Immunohistochemical analysis is extremely important for the diagnosis of SFTP: CD34, CD99, Vimentin, and BCL-2 are positively expressed, and expression of strong nuclear STAT6 is largely specific for SFT^[5]; whereas S-100 is negatively expressed.^[6]

Hiraoka et al^[7] believed that malignant SFTP should be considered in the presence of the following: abundant cells, crowded or overlapped nuclei, increased mitotic figures (>4/10 HPF), and significant changes in cell morphology. Because this tumor is often located close to the chest wall, surgical biopsy is relatively simple with few complications^[8]; however, Sung et al^[9]

Editor: Sergio Gonzalez Bombardiere.

The authors have no funding and conflicts of interest to disclose.

^a Department of Radiology, Shanghai Pulmonary Hospital, Tongji University School of Medicine, Shanghai, ^b Department of Radiology, The People's Hospital of Shihezi City, Shihezi, Xinjiang, ^c Tuberculosis Center for Diagnosis and Treatment, Shanghai Pulmonary Hospital, Tongji University School of Medicine, Yangpu, Shanghai, China.

* Correspondence: Yong Fang, Clinic and Research Center of Tuberculosis, Shanghai Key Lab of Tuberculosis, Shanghai Pulmonary Hospital, Tongji University School of Medicine, No. 507 Zhengmin Road, Yangpu District, Shanghai 200433, China (e-mail: 13916239320@163.com)

Copyright © 2017 the Author(s). Published by Wolters Kluwer Health, Inc. This is an open access article distributed under the Creative Commons Attribution-NoDerivatives License 4.0, which allows for redistribution, commercial and non-commercial, as long as it is passed along unchanged and in whole, with credit to the author.

Medicine (2017) 96:49(e9058)

Received: 8 February 2017 / Received in final form: 21 August 2017 / Accepted: 11 November 2017

<http://dx.doi.org/10.1097/MD.00000000000009058>

reported a success rate of only 43% for fine needle aspiration biopsy. We analyzed the possible causes of the low success rate of biopsy. First, the amount of aspirated tissue may be too small for microscopic observation or immunohistochemical examination. Second, the area biopsied may have been cystic or necrotic. (For this reason, with sufficient tissue quantity, the use of CT examination to identify obvious areas of enhancement is recommended for aspiration biopsy.) Third, SFTPs are generally large with a heterogeneous composition such that malignant tissue may only account for a small area of the tumor. Therefore, biopsy often has little value for distinguishing between malignant and benign tumors.^[10]

The ability to identify characteristics which differentiate benign and malignant tumors on CT evaluation before surgery is important for guiding clinical treatment. Most of the literature emphasizes the difficulty in differentiating between benign and malignant SFTPs by CT, but Song et al^[11] found that areas of low density and irregular pleural thickening are more common in malignant cases. Helage et al^[12] suggested that malignant SFTP is usually associated with a maximum tumor diameter >10 cm and a more abundant blood supply than benign SFTP. Accordingly, this retrospective analysis included 60 cases of SFTP confirmed by surgical pathology in Shanghai Pulmonary Hospital (affiliated with Tongji University), and evaluated tumor characteristics on preoperative CT examinations of patients with subsequently resected SFTP.

2. Materials and methods

2.1. Subjects

The study was approved by the Hospital Ethics Committee of Shanghai Pulmonary Hospital, Tongji University. There were 66 cases of SFT confirmed by surgical pathology diagnosed at Shanghai Pulmonary Hospital (affiliated to Tongji University) from July 2008 to December 2015 (64 cases from the pleura, 1 case each from the mediastinum and lung). There were 60 cases (28 males and 32 females) with complete clinical data included in this study, ages 25 to 80 years (average age: 56.5 ± 10.3 years). For 29 cases, clinical manifestations (fever, cough, chest pain, and respiratory distress) were present, whereas, 31 cases were reportedly asymptomatic at diagnosis. Occasionally, tumors were found on imaging examinations obtained for other diseases.

2.2. CT examination methods and image analyses

A Philips 40-layer or Siemens 64-layer spiral CT scanner was used for examinations performed with continuous scanning from apex pulmonis to basis pulmonis (5 mm layer thickness and spacing, and 1 or 0.6 mm reconstruction thickness). Of the study cases, 9 received CT plain scanning (8 benign SFTP and 1 malignant SFTP), 46 underwent enhanced CT scanning, and only 6 cases underwent both plain and enhanced CT scanning. To allow a multidimensional observation, data were transferred to a professional workstation for multiplanar reconstruction (MPR), maximum density projection (MIP) reconstruction, and volume rendering (VR). Observations made included the tumor location, morphology, size, border characteristics, density and pattern (homogeneity vs. heterogeneity, calcifications, intratumor blood vessels, etc.), and features of adjacent tissues. The morphologies were classified as mounded or mushroom umbrella shape, or quasicircular or oval shape, and growth resembling a casting mould in the chest (i.e., the mass grew along and filled

costophrenic or cardiaphragmatic angle). The borders were classified as either clear boundary or partially coarse boundary (i.e., no clear delineation between a mass and its surrounding tissue for more than one-fourth of the mass's boundary). The tumor densities were classified as homogeneous or heterogeneous (i.e., low-attenuation areas in the mass).

2.3. Pathologic diagnosis criteria of malignant solitary fibrous tumors

Malignant solitary fibrous tumors of the pleura (MSFPs) were diagnosed according to the criteria reported by England et al^[4]: high cellularity; mitotic activity (more than 4 mitotic figures per 10 high-power fields); pleomorphism; hemorrhage; and necrosis. To diagnose MSFP, one or more of criteria 1 to 3 should be present.

2.4. Statistical analysis

All measurement data were expressed as mean ± standard deviation. SPSS 21 statistical analysis software package (IBM Corp, Armonk, NY) was used for statistical processing. The independent samples *t* test was used for comparing the means for benign and malignant SFTP groups, and the chi-squared test was used for comparing frequency data. *P* > .05 was considered statistically significant.

3. Results

3.1. CT performance

The tumor location, morphology, and features for the 60 study patients are shown in Table 1. On CT, the tumors were characterized by a mounded or mushroom umbrella-shape (19

Table 1
Computed tomography manifestations of 60 solitary fibrous tumor of the pleura patients.

Manifestations	Cases	%
Location		
Upper right thorax	13	21.7
Lower right thorax	18	30
Upper left thorax	7	11.7
Lower left thorax	22	36.7
Morphology		
Mounded or mushroom umbrella-shaped	19	31.7
Quasi-circular or oval	30	50
Growth like casting mould in the chest	12	20
The maximum diameter (1.1–18.9 cm)		
<5 cm	33	55
5–10 cm	14	23.3
>10 cm	13	21.7
Boundary		
Clear	57	95
Coarse	3	5
Density		
Homogeneous	27	45
Inhomogeneous	33	55
Calcification	6	10
Blood supply		
Intratumor blood vessels	12	23.5
Vasa vasorum	3	5.9

Blood supply only analyzed in the 51 contrast-enhanced cases.



Figure 1. Malignant solitary fibrous tumor of the pleura in a 69-year-old man with chest pain. Chest computed tomography scan shows a soft tissue mass with coarse boundary.

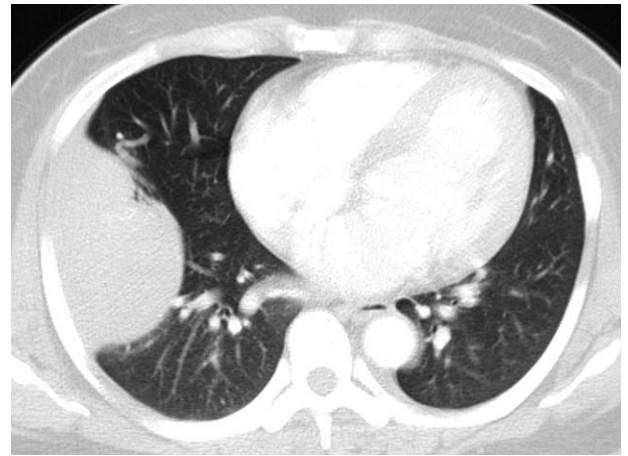


Figure 3. Benign solitary fibrous tumor of the pleura in an asymptomatic 37-year-old woman. Chest computed tomography scan reveals a mass in the right hemithorax with nourishing vessel originated from adjacent right middle lobe.

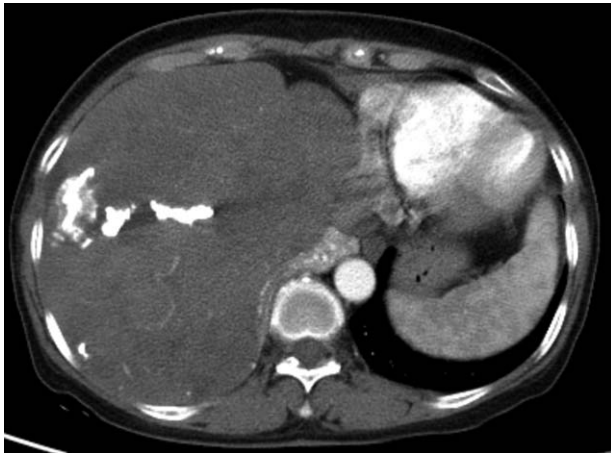


Figure 2. Malignant solitary fibrous tumor of the pleura in a 65-year-old woman with fever, cough, and dyspnea. Contrast-enhanced chest computed tomography scan (mediastinal window) demonstrates a heterogeneously enhancing soft-tissue mass in the right hemithorax with internal focal and linear areas of low attenuation, irregular strip calcification, and vessels.

cases) or quasi-circular or oval shape (30 cases), or by growth resembling a casting mould in the chest (12 cases, 2 of which extended into the interlobar fissures with a beak sign at the interlobular–pleural boundary). Fifty-seven cases had a clear boundary, and 3 had a partially coarse boundary (Fig. 1). The tumor sizes were varied, with a maximum diameter of 1.1 to 18.9 cm (average: 6.4 ± 4.8 cm). The tumor density was related to its

size, and 27 cases showed a homogeneous density, whereas the other 33 cases were inhomogeneous. The maximum diameters of the homogeneous cases were larger than 5 cm with irregular low-density necrotic areas, and areas with the appearance of a “geographic” pattern. Of the 33 inhomogeneous cases, which had areas of high and low density, there were 13 with a greatest diameter more than 10 cm. Six cases showed calcifications (Fig. 2), including linear or irregularly shaped ones. Multiple distorted blood vessels were observed within the tumor in 12 cases (Fig. 2). Thick nourishing peritumoral blood vessels were found in 3 cases (Figs. 3 and 4), originating from the adjacent bronchial artery, mediastinal bronchial artery, and phrenic artery, respectively.

Four cases had obvious regular or irregular pleura thickening around the tumor (Fig. 5); 2 cases compressed the adjacent ribs, causing absorption and cortical sclerosis (Fig. 5B); and 1 case was adjacent to the ribs, resulting in bony destruction and outward invasion to the chest wall muscles (Fig. 6). Furthermore, 4 cases had a small amount of lung tissue enfolded at the boundary of the tumor (Fig. 7), 2 cases had multiple peritumoral pulmonary bullae (Figs. 7 and 8), 18 cases were adjacent to lung tissue resulting in atelectasis, and 3 cases were associated with an obvious mediastinal shift to the contralateral side. Except for 1 case who complicated by lung cancer with an enlarged lymph node in the ipsilateral hilus pulmonis, no obvious lymph node or mediastinal enlargement was observed on CT. A small amount of effusion was found in the ipsilateral side of the chest in 9 cases. Five cases were complicated by lung cancer, 2 by tuberculosis, and 1 by granulomatous lesions.

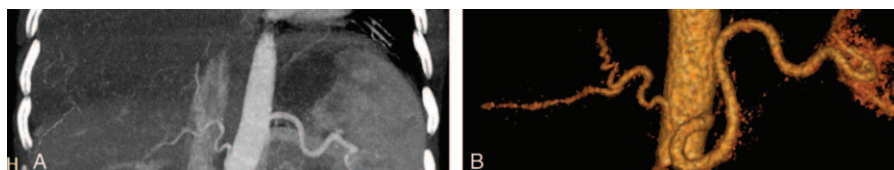


Figure 4. Malignant solitary fibrous tumor of the pleura in a 61-year-old woman with cough and dyspnea. Maximum density projection reconstruction and volume rendering images show an abnormally enlarged feeding artery branching from the phrenic artery.

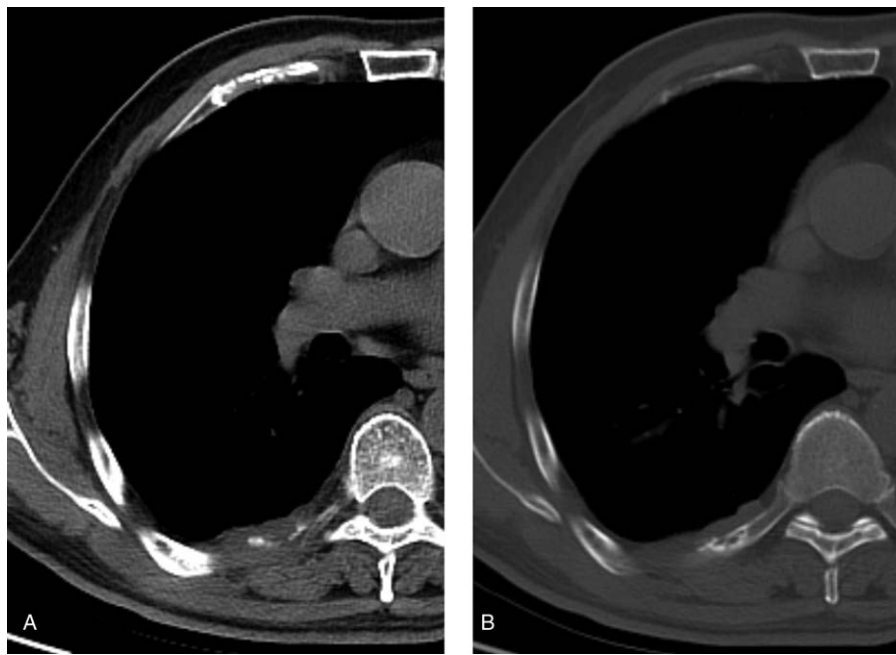


Figure 5. Benign solitary fibrous tumor of the pleura in an asymptomatic man. Chest computed tomography scan demonstrates a lower right pleural nodule, irregular thickening of the adjacent pleura, and bony absorption.

3.2. Surgical pathology results

Preoperative CT-guided percutaneous fine needle aspiration biopsy was performed on 10 patients. One case required 2 punctures. Microscopy revealed only a small amount of inflammatory and/or tissue cells in 8 cases such that a definitive diagnosis could not be made. Atypical cells were observed in only 1 case with malignant SFTP.

In general, masses were quasi-circular or lobulated and moderate to tough in texture, with areas of grayish-white, -yellow, or -black color. Microscopically, tumor cells were fusiform and interlaced with long fusiform nuclei, some with

visible nucleoli. A generous amount of collagenous fibers were deposited in the mesenchyme, and collagen was found in the adjacent pleural in 2 cases. Benign SFTP was diagnosed in 49 cases, and malignant SFTP in 11 cases. No SFTP metastases were found in the mediastinal or hilar lymph nodes.

3.3. Correlation of pathology with CT signs

Table 2 shows that, compared with benign SFTP, malignant tumors were greater in size and had a higher percentage rate of inhomogeneous density, intratumor blood vessels, and pleural effusions. No statistical differences were found for the presence of calcifications, pleural thickening, or rib changes.



Figure 6. A 58-year-old man with cough, dyspnea, and chest pain. Axial computed tomography demonstrates a malignant solitary fibrous tumor of the pleura in lower left pleural, with outward invasion to left chest wall muscles, a coarse boundary adjacent to ribs, and spot-like calcifications along the inner margin.

4. Discussion

SFTP is a kind of borderline tumor: most are benign with malignant or potentially malignant cases accounting for only about 10% to 15%.^[4] In this study, 11 cases (18.3%) were malignant, and the other 49 cases were benign, which is a slightly higher rate of malignancy than reported in the literature. Symptoms at diagnosis are seen in 54% to 67% of benign and 75% of malignant SFTPs.^[13] Because most SFTPs grow slowly and there is a great amount of compensatory space between the chest and lung, tumors are occasionally an incidental finding on physical or other examinations, and are often very large when found. Large tumors may compress the trachea and lung tissue, causing cough, chest tightness, dyspnea, and even respiratory insufficiency.^[14–17] Chest pain is common when the tumor arises from the parietal pleura, and if the tumor invades adjacent tissue structures and erodes lung tissue or ribs and nearby nerves, chest pain is more severe and hemoptysis may occur. Robinson^[18] reported that about 10% of their SFTP study patients developed paraneoplastic syndromes, such as hypertrophic osteoarthropathy, hypoglycemia, clubbed nail-

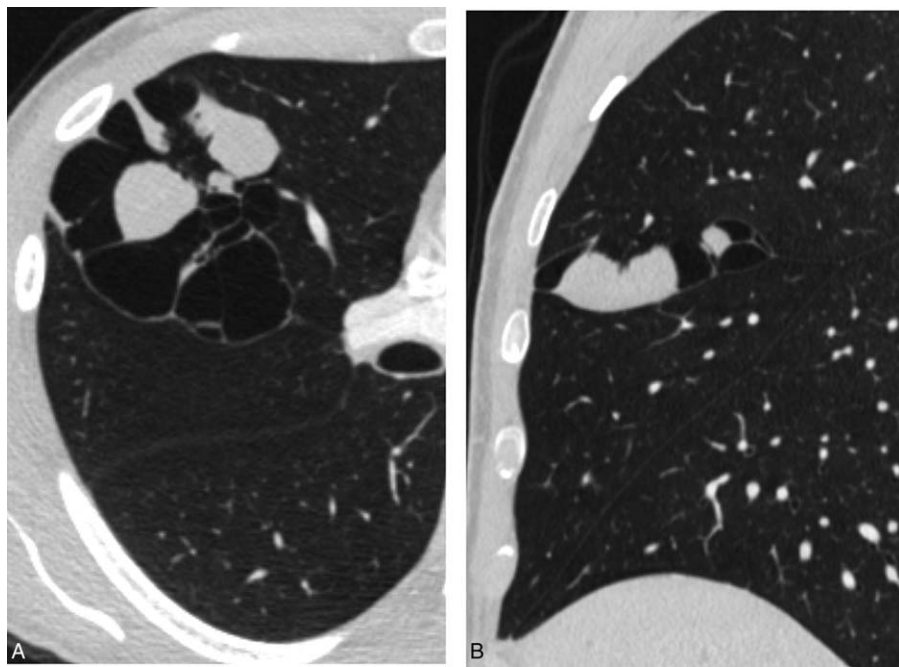


Figure 7. Benign solitary fibrous tumor of the pleura in an asymptomatic man. Chest CT scan demonstrates a cystic-solid nodule on the right horizontal fissure. Sagittal CT image shows a small amount of lung tissue enfolding on the superior border. CT = computed tomography.

beds, and gynecomastia or galactorrhea. Interestingly, they found the larger the tumor, the higher the probability of paraneoplastic syndromes. Hypertrophic osteoarthropathy was most common, with an incidence of about 22%; whereas hypoglycemia was rare (approximately 3% incidence). These paraneoplastic syndromes gradually disappeared after tumor resection, and their reappearance indicated tumor recurrence. In

our study, about half of the cases were incidentally found on physical examination or chest radiography obtained for unrelated reasons and symptoms include fever, cough, chest tightness, and other nonspecific manifestations. No patients had a paraneoplastic syndrome, and there was not a statistical difference in the incidence of symptoms between benign and malignant SFTP.

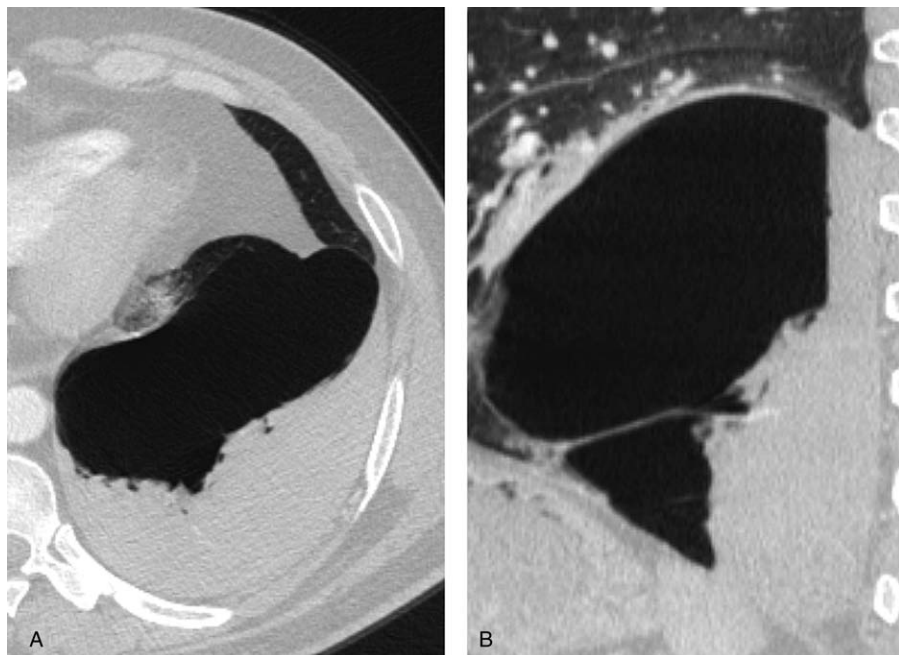


Figure 8. Computed tomography images of a benign solitary fibrous tumor of the pleura in a 52-year-old man with chest pain. Multiple pulmonary bullae are evident in the peritumoral lung tissue.

Table 2**Comparison of clinical features and CT signs in benign and malignant solitary fibrous tumor of the pleuras.**

	Benign SFT (n = 49)	Malignant SFT (n = 11)	P
Age, y	55.4 ± 9.9	61.5 ± 11.2	.07 ($t = -1.82$)
Gender			.18 ($\chi^2 = 0.67$)
Male	24	4	
Female	25	7	
Symptoms			.14 ($\chi^2 = 2.13$)
Yes	21	8	
No	28	3	
The maximum diameter, cm	5.4 ± 4.2	10.9 ± 4.6	<.001 ($t = -3.84$)
Density			.001
Homogeneous	27 (55.1%)	0 (0%)	
Inhomogeneous	22 (44.9%)	11 (100%)	
Calcification	4 (8.2%)	2 (18.2%)	.66 ($\chi^2 = 0.20$)
Intratumor blood vessels	6 (14.6%)	6 (60%)	.009 ($\chi^2 = 6.85$)
Pleural thickening	2 (4.1%)	2 (18.2%)	.31 ($\chi^2 = 1.05$)
Pleural effusion	4 (8.2%)	5 (45.5%)	.008 ($\chi^2 = 7.09$)
Rib changes	2 (4.1%)	1 (9.1%)	.46

Evaluation for the presence of intratumor blood vessels using contrast-enhanced CT was only performed in 41 of the benign and 10 of the malignant cases.

CT = computed tomography, SFT = solitary fibrous tumor.

Due to the abundant blood vessels on the surface of the tumor, the risk of bleeding with aspiration biopsy is high, and the tissue sample obtained from fine-needle aspiration is often too small to make a pathological diagnosis.^[19] Ten patients in our study had preoperative CT-guided aspiration biopsies, but a clear histodiagnosis was not obtained in 8 cases. A small number of atypical cells were observed in only 1 case of malignant SFT. Therefore, we believe that aspiration biopsy has little utility for diagnosis in SFT.

Multislice computed tomography (MSCT) can produce multidimensional reconstructions and show the location, morphology, density, and enhancement characteristics of a tumor. In addition, noninvasive vascular imaging can reveal the feeding arteries and tumor blood supply, as well as the relationships between a tumor and adjacent structures. The primary treatment for SFT is complete surgical resection, which has a good prognosis, and a second surgical resection should be performed for recurrence.^[20] For large tumors with abundant blood supply and feeding arteries visible on MSCT angiography, interventional embolization therapy followed by surgical resection can be considered to decrease bleeding and other risks associated with standard resection techniques.^[21] Benign lesions may also recur and metastasize, and histopathological results cannot definitively exclude malignancy; therefore, long-term follow-up is necessary for all surgical patients.^[14,22]

SFT are pleural tumors that may grow at any location in the chest. The positioning of large SFTs is often complex. For most pleural tumors, including SFTs, at least one side of the tumor intersects with the chest wall at an obtuse angle.^[18] Dedrick et al^[23] suggested that the gradual tapering of a pleural tumor near the lung, which was present in 11 cases in their series, is an important sign. They proposed that the formation of this sign was due to a wide-based attachment to the pleura along with growth similar to a casting mould in the chest. Some pedunculated tumors attach to one side of the pleura, or may connect with several different sites on the pleura, with rich nourishing blood vessels.^[3,4,18,24] The presence of a pedicle is characteristic of

extra-pulmonary tumors and very useful for localization diagnosis. No clearly pedunculated tumors were seen in our study. This may be related to the large tumor sizes or to our not recognizing the signs of a pedunculated tumor on CT.

Small SFTs (<5 cm) have homogeneous intensities, similar to muscle, with a CT value of approximately 30 to 60 HU. The larger the tumor, the greater the likelihood of inhomogeneous density. Giant SFTs have inhomogeneous intensities, caused by myxoid or cystic degeneration, hemorrhage, or necrosis; however, complete cystic degeneration has yet to be reported. Calcification is seen less commonly and is primarily manifested as a punctate-, strip-, or coarse plaque-like lesion of high density. Calcifications are also more likely to be found in larger tumors.^[4,6] No studies have reported that calcification is associated with malignancy. In this study, 6 cases (10%) had calcification, including 3 giant tumors, with obvious areas of low-density representing necrosis on CT. The remaining 3 cases were relatively smaller tumors with homogeneous density on CT, but necrosis was apparent under microscopy.

Mild-to-moderate homogeneous enhancement can be observed in small tumors on contrast-enhanced CT, but is rare in the presence of tumor blood vessels. Patchy inhomogeneous enhancement is common in giant SFTs with enhancement scanning, and delayed enhancement is seen in some regions, producing a characteristic “geographic” enhancement pattern.^[25] The larger the tumor, the more inhomogeneous the enhancement.

SFTs have rich blood supply, and thick tortuous tumor blood vessels are often visible within the tumor.^[24] In this study, blood vessels were clearly seen in 12 cases (23.5%). Nourishing blood vessels usually originate from the phrenic, intercostal, and internal mammary, and part of the bronchial arteries. In this study, CT showed thick peritumoral feeding arteries in 3 cases, originating from the right pulmonary bronchial artery, the left mediastinal bronchial artery, and the right phrenic artery. Reports from imaging research on the origin of feeding blood vessels are lacking in the literature: in this study, we applied MIP and VR in an attempt to gain more useful information that would be helpful for treatment management.

Grossly, most SFTs appear well-encapsulated. The fat layer subjacent to the parietal pleura that is adjacent to tumor is often clear. In addition, compression of the lung tissue can occur resulting in atelectasis. Similar to pseudocapsule which has a clear boundary, the parenchymal phase is significantly enhanced on contrast-enhanced scans, in contrast to pulmonary infiltration. Notably, a small amount of adjacent lung tissue was clearly enfolded in the tumor tissue in 4 of our study cases. In 1 case, the tumor arose from the pleura overlying the right horizontal fissure, and multiple air-filled cavities were visible in adjacent lung tissue; this resulted in the false appearance of cystic–solid lesions with solid tumor nodules, which was misdiagnosed as congenital cystic adenomatoid malformation by the preoperative CT. In another case, the SFT grew like casting mould in the chest, and large-scale pulmonary bullae were observed in the adjacent lung tissue. Bullae have been reported in other studies,^[26] and may be related to bronchial check-valve obstruction caused by lung tissue being wrapped by tumor.

Some scholars believe that malignancy is suggested by the presence of a maximum tumor diameter >10 cm, inhomogeneous density, rich blood supply, obscure boundaries, peripheral pleural thickening, and pleural effusion.^[11,19] Our study also showed that the 11 cases of borderline or malignant SFTs had larger volumes (with an average maximum diameter of 10.9 cm),

inhomogeneous intensities and irregular “flaky” low-density areas, rich intratumor blood vessels, geographic pattern enhancement, and a high incidence of pleural effusion. However, no difference in pleural thickening was found between benign and malignant SFTPs. Two cases were noted to have regular or irregular pleural thickening around the tumors. In one of the cases, rib absorption subjacent to irregular pleural thickening and associated with an obscure boundary was found. The tumor was initially misdiagnosed as malignant by preoperative CT, but was shown to be a benign SFTP with adjacent pleural collagen fiber hyperplasia on pathology after surgery. We speculate that the CT findings may have been related to local inflammation caused by changes in surrounding anatomical structures triggered by the mass.

The differential for SFTP includes pleural mesothelioma, isolated pleural metastasis, neurogenic tumor, intrapulmonary tumor, and solid mass pulmonary sequestration. A brief description of each of these will follow: Benign pleural mesothelioma is generally small and difficult to distinguish from SFTP on CT images. Clinically, most pleural mesothelioma patients have a history of asbestos exposure, which is usually lacking in SFTP patients. Malignant pleural mesothelioma typically shows a diffuse infiltrative growth pattern characterized by widespread, nodular pleural thickening mainly of the parietal pleura, but it also may involve the visceral pleura and pericardium as well, and is often accompanied by pleural effusion. Isolated pleural metastases are small lesions, often accompanied by limited adjacent pleural thickening and pleural effusion. Diagnosis of the primary lesion allows this to be distinguished from SFTP. Neurogenic tumors show obvious enhancement on contrast CT without tortuous intratumor blood vessels, and generally occur in a nerve zone. They are most commonly seen on intercostal or spinal nerves, with the former passing along the course of an intercostal nerve, and the latter located near the posterior mediastinal spine with a “dumbbell-like” appearance. Neurogenic tumors can compress and invade adjacent ribs or vertebral bodies, resulting in enlargement of the intervertebral foramen. On the other hand, it is relatively rare to find bone changes with SFTP. Only 3 cases in our study had bone changes evident in peritumoral ribs. Intrapulmonary tumors include peripheral lung cancer or pulmonary sarcoma, and are important to distinguish from SFTP. Peripheral lung cancer is commonly characterized by lobulation, a short burr sign, cavitation, tubule and pleural indentation, mediastinal and hilar lymph node enlargement, and an acute intersecting angle with the pleura; whereas SFTP typically has a wide-based attachment to the pleura and a smooth boundary. Pulmonary sarcoma shows expansive growth, generally being a larger mass with a cavity and calcification in its center, but usually limited pleural invasion. SFTP, in contrast, is close to the pleura with a maximum diameter located in the chest, and compression of adjacent lung tissue. It is not easy to distinguish SFTP originating from the interlobar fissure from a parenchymal mass, although the interlobular pleural “tail” sign and fusiform appearance on MPR can suggest the lesion originates from the pleura.^[27] Solid mass pulmonary sequestrations are often located in the basal segment of the lower lobes, with abnormal arterial blood supply usually originating from the thoracic aorta or an abdominal aortic branch, but sometimes from the inferior phrenic artery, intercostal artery, and other arterial source. In this study, 1 SFTP case with large vessels from the right middle lobe seen to enter the tumor on CT and grossly, was intraoperatively misdiagnosed as pulmonary sequestration. Further careful observation,

however, revealed that the tumor was located in the pleura. Clinically, solid mass pulmonary sequestration often has a history of recurrent infections and can be resected when identified.

In conclusion, SFTP is a rare soft tissue tumor, which is often very large when found. It is difficult to make an accurate diagnosis based on imaging and clinical presentation. MSCT imaging reveals certain characteristics: extra-pulmonary location, casting mould-like growth in the chest, a rich blood supply, a strong geographic enhancement pattern, and common tumor blood vessels. Large tumor size, inhomogeneous density, abundant intratumor blood vessels, and pleural effusion all suggest the possibility of malignancy. MSCT can clearly show feeding arteries and provide a great amount of valuable information for preoperative diagnosis and to help guide surgical management.

References

- [1] Migliore M, Okateya V, Calvo D, et al. Two cases of giant solitary fibrous tumor of the pleura: a not-so-rare tumor? *Asian Cardiovasc Thorac Ann* 2014;22:226–8.
- [2] Cardillo G, Facciolo F, Cavazzana AO, et al. Localized (solitary) fibrous tumors of the pleura: an analysis of 55 patients. *Ann Thorac Surg* 2000;70:1808–12.
- [3] Briselli M, Mark EJ, Dickersin GR. Solitary fibrous tumors of the pleura: eight new cases and review of 360 cases in the literature. *Cancer* 1981;47:2678–89.
- [4] England DM, Hochholzer L, McCarthy MJ. Localized benign and malignant fibrous tumors of the pleura. A clinicopathologic review of 223 cases. *Am J Surg Pathol* 1989;13:640–58.
- [5] Demicco EG, Harms PW, Patel RM, et al. Extensive survey of STAT6 expression in a large series of mesenchymal tumors. *Am J Clin Pathol* 2015;143:672–82.
- [6] de Perrot M, Fischer S, Brundler MA, et al. Solitary fibrous tumors of the pleura. *Ann Thorac Surg* 2002;74:285–93.
- [7] Hiraoka K, Morikawa T, Ohbuchi T, et al. Solitary fibrous tumors of the pleura: clinicopathological and immunohistochemical examination. *Interact Cardiovasc Thorac Surg* 2003;2:61–4.
- [8] Ali SZ, Hoon V, Hoda S, et al. Solitary fibrous tumor. A cytologic-histologic study with clinical, radiologic, and immunohistochemical correlations. *Cancer* 1997;81:116–21.
- [9] Sung SH, Chang JW, Kim J, et al. Solitary fibrous tumors of the pleura: surgical outcome and clinical course. *Ann Thorac Surg* 2005;79:303–7.
- [10] Miyoshi K, Okumura N, Kokado Y, et al. Solitary fibrous tumor of the pleura with a minute malignant component and diaphragmatic vascular supply: report of a case. *Surg Today* 2008;38:344–7.
- [11] Song SW, Jung JI, Lee KY, et al. Malignant solitary fibrous tumor of the pleura: computed tomography-pathological correlation and comparison with computed tomography of benign solitary fibrous tumor of the pleura. *Jpn J Radiol* 2010;28:602–8.
- [12] Helage S, Revel MP, Chabi ML, et al. Solitary fibrous tumor of the pleura: can computed tomography features help predict malignancy? A series of 56 patients with histopathological correlates. *Diagn Interv Imaging* 2016;97:347–53.
- [13] Thway K, Ng W, Noujaim J, et al. The current status of solitary fibrous tumor: diagnostic features, variants, and genetics. *Int J Surg Pathol* 2016;24:281–92.
- [14] Abe M, Nomori H, Fukazawa M, et al. Giant solitary fibrous tumor of the pleura causing respiratory insufficiency: report of 3 cases. *Ann Thorac Cardiovasc Surg* 2014;20(suppl):441–4.
- [15] Magdeleinat P, Alifano M, Petino A, et al. Solitary fibrous tumors of the pleura: clinical characteristics, surgical treatment and outcome. *Eur J Cardiothorac Surg* 2002;21:1087–93.
- [16] Cardillo G, Carbone L, Carleo F, et al. Solitary fibrous tumors of the pleura: an analysis of 110 patients treated in a single institution. *Ann Thorac Surg* 2009;88:1632–7.
- [17] Lococo F, Cesario A, Cardillo G, et al. Malignant solitary fibrous tumors of the pleura: retrospective review of a multicenter series. *J Thorac Oncol* 2012;7:1698–706.
- [18] Robinson LA. Solitary fibrous tumor of the pleura. *Cancer Control* 2006;13:264–9.

- [19] Cardillo G, Lococo F, Carleo F, et al. Solitary fibrous tumors of the pleura. *Curr Opin Pulm Med* 2012;18:339–46.
- [20] Milano MT, Singh DP, Zhang H. Thoracic malignant solitary fibrous tumors: a population-based study of survival. *J Thorac Dis* 2011; 3:99–104.
- [21] Aydemir B, Celik S, Okay T, et al. Intrathoracic giant solitary fibrous tumor. *Am J Case Rep* 2013;14:91–3.
- [22] Harrison-Phipps KM, Nichols FC, Schleck CD, et al. Solitary fibrous tumors of the pleura: results of surgical treatment and long-term prognosis. *J Thorac Cardiovasc Surg* 2009;138:19–25.
- [23] Dedrick CG, McLoud TC, Shepard JA, et al. Computed tomography of localized pleural mesothelioma. *AJR Am J Roentgenol* 1985;144: 275–80.
- [24] Asai K, Suzuki K, Shimota H, et al. Solitary fibrous tumor of the pleura with hemothorax at the thoracic apex. *Jpn J Thorac Cardiovasc Surg* 2003;51:434–7.
- [25] Cardinale L, Allasia M, Ardisson F, et al. CT features of solitary fibrous tumour of the pleura: experience in 26 patients. *La Radiol Med* 2006;111:640–50.
- [26] Baek JE, Ahn MI, Lee KY. Solitary fibrous tumor of the pleura manifesting as an air-containing cystic mass: radiologic and histopathologic correlation. *Korean J Radiol* 2013;14:981–4.
- [27] Cardinale L, Cortese G, Familiari U, et al. Fibrous tumour of the pleura (SFTP): a proteiform disease. Clinical, histological and atypical radiological patterns selected among our cases. *La Radiol Med* 2009;114:204–15.